Recent progress in developing non-noble metal-based photocathodes for solar green hydrogen production

Recent Progress in Developing Non-Noble Metal Based Photocathodes for Solar Green Hydrogen Production

Antony Charles Minja[a,b], Karthick Raj AG[a,b], Arno Raes[a,b], Rituraj Borah[a,b] and Sammy W. Verbruggen[a,b]*

[a] Sustainable Energy, Air & Water Technology (DuEL), Department of Bioscience Engineering, University of Antwerp, Groenenborgerlaan 171, 2020 Antwerp, Belgium

[b] NANOlab Center of Excellence, Groenenborgerlaan 171, 2020 Antwerp, Belgium

Email: Sammy.Verbruggen@uantwerpen.be;

Abstract

Photocathodes play a vital role in photoelectrocatalytic water splitting by acting as catalysts for reducing protons to hydrogen gas when exposed to light. Recent advancements in photocathodes have focused on addressing the limitations of noble metal-based materials. These noble metal-based photocathodes rely on expensive and scarce metals such as platinum (Pt) and gold (Au) as co-catalysts or ohmic back contacts, respectively, rendering the final system less sustainable and costly when applied at scale. This mini-review summarizes the important recent progress in the development of non-noble metal-based photocathodes and their performance in the hydrogen evolution reaction (HER) during photoelectrochemical water splitting. These advancements bring non-noble metal-based photocathodes closer to their noble metal-based counterparts in terms of performance, thereby paving the way forward towards industrial-scale photo-electrolysers or photoelectrochemical cells for green hydrogen production.

Keywords: Non-noble metal photocathodes, solar green hydrogen production, photoelectrochemical water splitting, sustainable energy, renewable energy

1. Introduction

In view of the current state-of-the-art, the most technologically mature route to produce solar green hydrogen is electrolysis powered by renewable electricity (photovoltaics (PV) or wind). As both electrolysis and PV are two market-ready technologies, the majority of the green hydrogen projects implement an integrated system of the two (**Figure 1 (a)**) [1]. However, for green hydrogen to become a mainstream fuel and chemical raw material, the cost of hydrogen production has to be lowered significantly from the current >5$ per kg to <2 $ per kg [2]. In that perspective, direct photoelectrochemical (PEC) water splitting for hydrogen production is gaining increasing importance (**Figure 1 (b)**). Firstly, the direct conversion of solar energy and water into hydrogen and oxygen in PEC cells excludes extra PV systems. This process occurs at the semiconductor-electrolyte interface, where the semiconductor photoelectrodes absorb solar energy that leads to the excitation of electrons from the valence band to the conduction band generating electron-hole pairs. This creates a potential difference between the photoelectrodes and the electrolyte solution driving the redox reactions involved in water splitting. The electrons are then transported to the cathode, where they reduce protons (H^+) in water to form hydrogen gas (H_2). Simultaneously, the holes are transported to the anode, where they oxidize water molecules (H_2O) to produce oxygen gas (O_2). The use of earth-abundant non-noble metal based photoelectrodes is not only significantly cheaper but can also be advantageous from a stability and maintenance point of view. Although PEC water splitting could be at the basis of a new generation of green hydrogen production technologies [3, 4] its large-scale practical implementation (*i.e.*, going all the way up to megawatt (MW) scale) is generally considered to be hindered by mainly the poor durability of photoanodes, that catalyse the oxygen evolution reaction (OER) [5]. It should be noted though, that photocathodes, which catalyse the hydrogen evolution reaction (HER), also largely suffer from photocorrosion and poor reaction kinetics [6]. While much research has focused on improving the sluggish OER

kinetics by modifying photoanodes, less attention has been paid to photocathodes, even though they are an equally critical component in the full system. This review aims to highlight recent efforts (*i.e.,* limited to the past five years) to improve photocathodes utilizing earth-abundant materials for sustainable hydrogen production through PEC water splitting.

Photocathodes, by virtue of being *p*-type semiconductor materials, generate holes as the primary charge carriers under solar illumination in parallel to *n*-type photoanodes that aim at generating electrons. This brings about a potential difference that drives a photocurrent in the external circuit, thereby facilitating HER at the cathode and OER at the anode, respectively (**Figure 1 (c)**). To achieve efficient hydrogen production, it is crucial to have high HER efficiency and selectivity, which largely depends on the properties of the photocathode material, including its band structure, electronic conductivity, and surface characteristics [7-9] shown in **Figure 1 (c)** and **(d)**, what makes the fabrication of a photocathode challenging is the fact that the photocathode has to fulfil two primary requirements in its band structure. Firstly, the band gap of the photocathode must be sufficiently smaller than that of the photoanode so that the low energy part of the solar spectrum that transmits through the photoanode can still excite electrons in the photocathode (unless a reactor design is employed wherein both photoelectrodes are illuminated from both sides). Secondly, the alignment of the bands should be such that the Fermi-level of the photoanode is higher than the Fermi-level of the photocathode in order for the electrons to flow in the direction as shown. Thus, the development of photocathodes meeting these criteria to complement the photoanodes is inherently challenging from the perspective of fundamental material properties. When one also considers the surface catalytic activity (often imparted by a co-catalyst) and chemical stability required for the entire electrochemical process to take place, it becomes increasingly challenging. This work critically reviews recent advances in photocathode development for PEC water splitting without the use of noble metals. The focus of this review is exclusively on recent reports on

photocathodes that demonstrate promising performance even without the incorporation of noble metals.

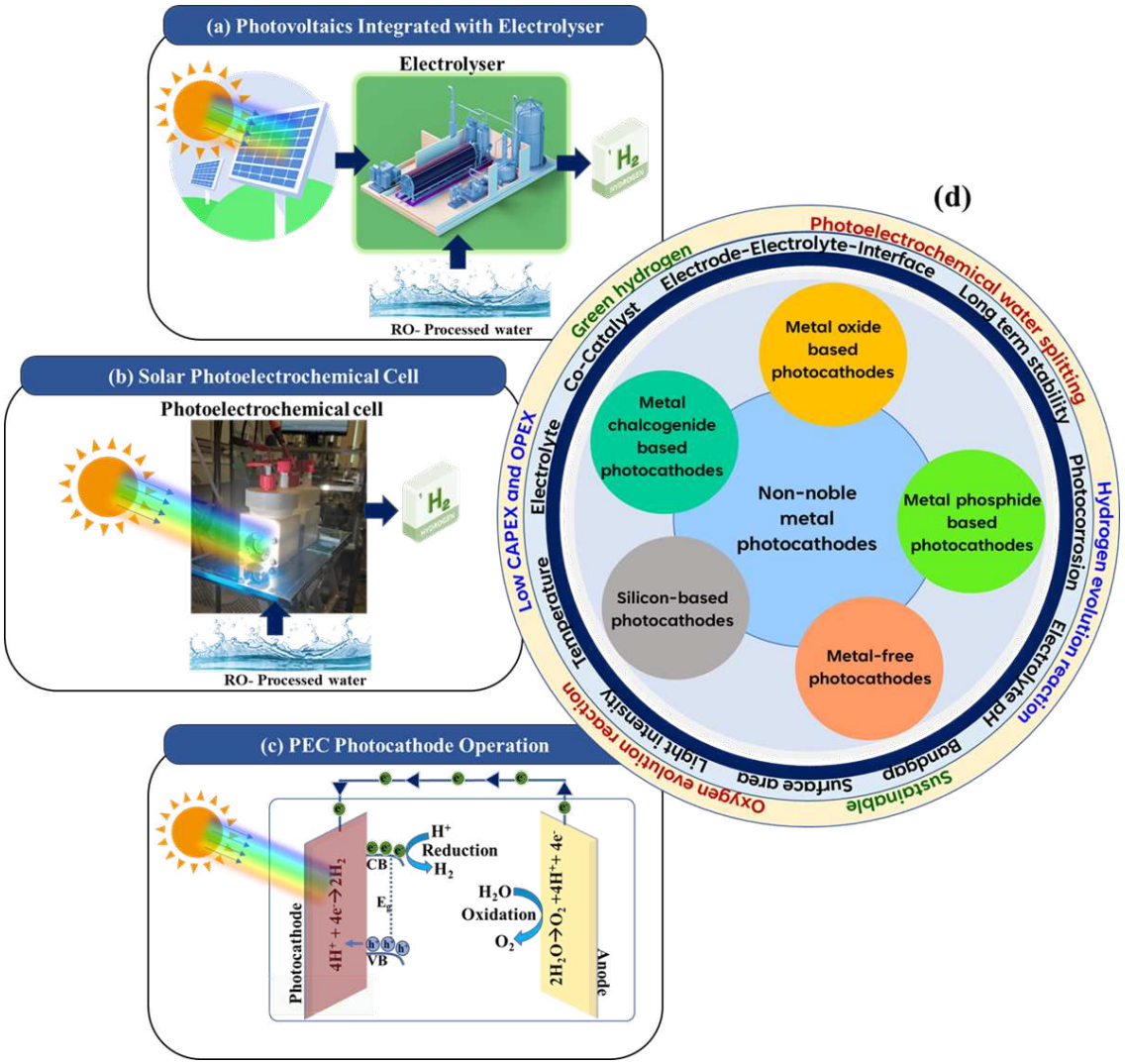

Figure 1. **(a)** Presently employed systems that combine electrolysers and photovoltaic technology to generate green hydrogen from solar energy. **(b)** Photoelectrochemical cells operating directly under sunlight without requiring photovoltaic panels. **(c)** Schematic showing the operation of a photocathode in a PEC cell. **(d)** Schematic illustration of various non-noble metal-based photocathodes, categorized by their material composition. It also showcases influencing experimental parameters and advantages of PEC water splitting in the inner and outer rings, respectively.

Over the years, noble metal-based photocathodes, particularly those incorporating platinum (Pt) [10] and Ruthenium (Ru) in the form of RuO_x as co-catalyst [11], have been extensively utilized in PEC hydrogen production and water splitting due to their excellent catalytic activity and stability. For instance, a study conducted by Chen *et al.* demonstrated a Pt-based photocathode with an earth-abundant semiconductor multi-junction composed of

$Cu_2O/ZnO/TiO_2$ as the photo-absorber, achieving a high photocurrent density of 8.2 mA cm^{-2} [12]. Another study by Tong *et al.* introduced a Pt_1/N–Ni co-catalyst integrated into a Cu_2O photocathode, which not only enhanced charge transfer kinetics at the electrode-electrolyte interface but also reduced the overpotential for hydrogen evolution. This resulted in an impressive photocurrent density of 11.9 mA cm^{-2} at 0 V *vs* RHE [13]. These investigations demonstrate that co-catalysts effectively lower the required overpotential for hydrogen evolution, thereby improving the overall efficiency and stability of the photocathode. Additionally, various semiconductor photocathode designs such as those of copper including oxides [14], sulfides [15], and others [16] have employed thin gold (Au) films as back contacts between the semiconductor layer and the substrate. These gold films serve the dual purpose of reflecting transmitted light for enhanced energy utilization, and charge collection, facilitating efficient charge separation, improved charge transfer kinetics, and overall long-term stability.

The use of non-noble metal-based materials in the construction of photocathodes, serving different functions such as HER co-catalysts, protective layers, and hole selective layers, is essential for shifting from costly and scarce noble metal-containing photocathodes in water splitting and hydrogen production. Efficient and practical alternative designs and constructions of photocathodes should possess desirable characteristics such as high photocurrent density, low onset potential and overpotential, and good stability. However, the other side of the medal is that non-noble metal-based photocathodes can be vulnerable to corrosion and degradation [17, 18]. To address this challenge, researchers have explored various strategies, including co-catalyst impregnation [7], surface modification [19], doping [20], and heterojunction fabrication [21], to enhance the stability and catalytic activity of non-noble metal-based photocathodes.

2. Non-noble metal-based photocathode architectures

The increasing demand for sustainable hydrogen production has sparked a shift towards development of non-noble metal-based photocathodes rather than their noble metal counterparts. This transition is driven by the abundance, cost-effectiveness, tuneable properties, stability, and environmental advantages of non-noble metal materials, particularly as we envision large-scale hydrogen production applications. Recent advances in non-noble metal-based photocathodes for water splitting and hydrogen production can be categorized based on the primary semiconducting material, as depicted in graphical scheme **Figure 1 (d)**. **Table 1** provides a summary of all non-noble metal-based photocathode architecture covered in this review. Subsequent sections that correspond to the earlier scheme categorisation, will delve into the specific roles played by different non-noble metal materials integrated into these photocathodes and how they contribute to improved performance.

Table 1. An overview of all non-noble metal-based photocathode studies presented in this review.

Photocathode	Co-catalyst	Protective layer/ Hole transport layer	Method of preparation	Photocurrent density (mA/cm^2)	Electrolyte	Stability	ABPE (%)	IPCE (%)	STH (%)	Light source used	Ref
Metal oxide-based photocathodes											
Multi-junction NiO_x/**Cu_2O**/AZO/ MoO_x	MoO_x	AZO	Electrodeposition and RF magnetron sputtering	6.1 mA/cm^2 at 0 V *vs* RHE	1 M Na_2SO_4 + 0.1 M KPi (pH 4.9 ± 0.1)	6 h at 0 V	1.75 % at 0.5 V vs RHE	60 % at 300 to 500 nm	-	1 Sun	[22]
TiO_2/ZnO/**Cu_2O**	-	TiO_2/ZnO	Electrodeposition and dip coating	0.18 mA/cm^2 at -0.2 V *vs* Ag/AgCl	0.1M Na_2SO_4 (pH 6.8)	20 min at -0.2 V vs Ag/AgCl	-	-	-	2 Sun	[21]
Cu_2O/Ni-CuBTC	Ni-CuBTC	-	Electrodeposition and Hydrothermal	1.51 mA/cm^2 at 0 V *vs* RHE	0.5 M Na_2SO_4 + 0.2 M PBS (pH 5)	20 min at 0.5 V vs RHE	-	-	-	1 Sun	[7]
Cu_2O/MoS_2	-	MoS_2	Electrodeposition and spin coating	6.5 mA/cm^2 at -0.2 V *vs* RHE	0.5M Na_2SO_4 (pH 6.7)	1 h at 0 V vs RHE	-	27 % at 400 nm, 0.2 V vs RHE	-	1 Sun	[23]
Cu/Al/**Cu_2O**	-	Cu/Al	Thermal evaporation and electrodeposition	2.16 mA/cm^2 at 0 V *vs* RHE	0.1 M Na_2SO_4 (pH 7)	2 h at 0 V vs RHE	-	-	-	1 Sun	[4]
Co_3O_4	-	-	Hydrothermal	1.15 mA/cm^2 at -0.4 V *vs* Ag/Agcl	0.1 M H_2SO_4 (pH 1)	-	-	-	-	1 Sun	[24]
Co_3O_4/CuO	CuO	-	Electrodeposition	6.5 mA/cm^2 at -0.3 V *vs* SCE	0.5 M Na_2SO_4	30 min at 0 V	-	-	-	1 Sun	[25]

Photocathode	Co-catalyst	Protective layer/ Hole transport layer	Method of preparation	Photocurrent density (mA/cm^2)	Electrolyte	Stability	ABPE (%)	IPCE (%)	STH (%)	Light source used	Ref
Fe-Ni co-doped **Co_3O_4**	Co-doped Fe-Ni	-	Spray pyrolysis	13.6 mA/cm^2 at -1 V	0.3 M Na_2SO_4	1 h at -1 V	0.34 % at 0.28 V and 636 nm	42 % at 405 nm	11.37	1 Sun	[26]
Cu doped **NiO**	Cu	-	Sol-gel spin coating	6.97 mA/cm^2 at -1.5 V *vs* Ag/AgCl	0.1 M NaOH	-	-	-	-	30 w UV	[27]
Cu: NiO/**$CuBi_2O_4$**	-	Cu:NiO (HTL)	Spray pyrolysis and electron beam evaporation	2.83 mA/cm^2 at 0.6 V *vs* RHE	0.3 M K_2SO_4 +0.2 M phosphate buffer (pH 6.65)	2 h at 0.6 V vs RHE	-	40 % at 400 nm (0.6 V)	-	1 Sun	[28]
$CuBi_2O_4$/CuO	CuO	-	Electrodeposition	1.87 mA/cm2 at 0.6 V *vs* SHE	0.1 M NaOH (pH 13)	6 h at 0.6 V vs SHE	-	16 % at 400 nm	-	1 Sun	[29]
Metal Chalcogenide based photocathodes											
MoS_2/**Sb_2S_3**	-	MoS_2	Sublimation and Sputtering	10 mA/cm^2 at 0 V *vs* RHE	0.5 M Na_2SO_4 (pH 6.5)	2 h at 0.2 V vs RHE	-	33 % at 800 nm	-	1 Sun	[30]
MoS_2/TiO_2 nanorods	-	-	Hydrothermal	5.2 mA/cm^2 at -0.4 V *vs* RHE	0.35 M Na_2S + 0.25 M Na_2SO_3	5 cycles of 5h at -0.4 V vs RHE	-	-	-	1 Sun	[31]
Cu_2BaSnS_4	-	-	Solgel spin coating	6.805 mA/cm^2 at 0 V *vs* RHE	0.5 M Na_2S (pH 12.9)	-	10 % at 0.1 V	-	-	4.7 mW/cm^2 LED	[32]
Mo/**Cu_2BaSnS_4**	-	Mo	Sputtering and spin coating	4 mA/cm^2 at 0 V *vs* RHE	0.1 M Na_2SO_4 (pH 7)	2 h at 0 V vs RHE	-	-	-	1 Sun	[33]
Cu_2S/ZnO nanorods	-	ZnO	Hydrothermal	0.64 mA/cm^2 at 0 V *vs* RHE	1 M KCl (pH 5.97)	-	-	10.5 % at 450 nm	-	1 Sun	[34]

Photocathode	Co-catalyst	Protective layer/ Hole transport layer	Method of preparation	Photocurrent density (mA/cm^2)	Electrolyte	Stability	ABPE (%)	IPCE (%)	STH (%)	Light source used	Ref
ZnO/**Cu_2S**	-	ZnO	Electrodeposition, SILAR method	0.095 mA/cm^2 at 0 V *vs* Ag/AgCl	0.5 M Na_2SO_3 (pH 10)	-	-	-	-	1 Sun	[35]
Dimensions dependent **SnS** nanocrystals	-	-	Hot and cold injection method	160 $\mu A/cm^2$ at -0.085 V *vs* RHE	0.5 M H_2SO_4	-	-	2.74 % at 600 nm	-	1 Sun	[36]
Bi_2S_3-Cu_3BiS_3	-	-	CBD and spin coating	7.8 mA/cm^2 at 0 V *vs* RHE	0.5 M Kpi (pH 7)	21 h at 0 v vs RHE	1.83 % at 0.45 V	20 % at 500 nm	2.33	1 Sun	[37]
$CuInS_2$/MoS_2	-	MoS_2	Electrodeposition and sulfurization	8.74 mA/cm^2 at -0.1 V *vs* RHE	1M $HClO_4$ (pH 0.9-1.1)	-	-	Above 25 % at 400 to 700 nm	-	1 Sun	[38]
Metal phosphide-based photocathodes											
Co_2P- Si inverted pyramids-	-	-	Electrochemical etching and drop casting	35.2 mA/cm^2 at 0 V *vs* RHE	0.5 M H_2SO_4 (pH 0.3)	150 h at 0 V vs RHE	-	76 % at 600 nm	-	1 Sun	[39]
TiO_2/**GaP**		TiO_2	ALD		0.2 M PBS (pH 7)	-	-		-	405 nm LED 40-120 $\mu W/cm^2$	[40]
Silicon based photocathodes											
p-Si-NiFe codoped In_2S_3	NiFe- In_2S_3	-	Hydrothermal	80.9 mA/cm^2 at -1.3 V *vs* RHE	0.5 M Na_2SO_3	2 h at 0 V vs RHE	-	-	-	1 Sun	[41]
MoS_2/**p-Si**	MoS_2	-	Etching and in situ assembly	28.2 mA/cm^2 at 0 V *vs* RHE	0.5 M H_2SO_4 (pH 0.6)	60 h at 0 V vs RHE	-	-	-	1 Sun	[42]

Photocathode	Co-catalyst	Protective layer/ Hole transport layer	Method of preparation	Photocurrent density (mA/cm^2)	Electrolyte	Stability	ABPE (%)	IPCE (%)	STH (%)	Light source used	Ref
3D textured graphene/**p-Si**	Graphene	-	CVD and EVA graphene transfer	32.5 mA/cm^2 at 0 V *vs* RHE	1 M $HClO_4$ (pH 0)	80 h at -0.3 V	-	-	-	1 Sun	[43]
Metal-free photocathodes											
g-C_3N_4/WS_2 @rGONR_x	WS_2@rGO NR_x	-	Hydrothermal and thermal decomposition	47 mA/cm^2 at -0.7 V *vs* RHE	0.5 M H_2SO_4 (pH 1)	1 h at -0.6 V vs RHE	-	-	-	1 Sun	[44]
Cu- **Polymeric C_3N_4**	Cu	-	Thermal decomposition	200 µA/cm^2 at -0.42 V *vs* RHE	0.2 M Na_2SO_4 (pH 6.8)	1 h at -0.42 V vs RHE	-	-	-	1 Sun	[45]
Cu_2O/**g-C_3N_4**	-	-	Electrodeposition and dip coating	2.5 mA/cm^2 at 0 V *vs* RHE	0.1M Na_2SO_4 (pH 7)	-	-	-	-	1 Sun	[46]
$NiWO_4$/g-C_3N_4	$NiWO_4$	-	Thermal polycondensation and solvothermal	167.8 mA/cm2 at 0.048 V *vs* RHE	0.5 M H_2SO_4	10 h at 0.048 V vs RHE	25.5 % at 0.048 V vs RHE	-	-	300 W Xenon lamp at a distance of 5 cm	[47]

***Note**: **ABPE**- Applied bias photon to conversion efficiency; **IPCE**- Incident photon to conversion efficiency; **STH**- Solar to hydrogen efficiency; **1 Sun** = 100 mW/cm^2; **RHE**- Reversible hydrogen electrode; **SCE**- Saturated calomel electrode; **Ag/AgCl**- Silver-silver chloride reference electrode; **SHE**- Standard hydrogen electrode; **HTL**- Hole transport layer; **ALD**- Atomic layer deposition; **CBD**- Chemical bath deposition; **PBS** – Phosphate buffer solution;*

2.1. Metal oxide-based photocathodes

Copper and its oxide compounds are commonly utilized as photocathodes in PEC cells for water splitting. Two main forms of copper oxide, cuprous oxide (Cu_2O) and cupric oxide (CuO), are frequently studied due to their p-type semiconductor properties. Cu_2O has particularly received extensive attention as a photocathode material, with a bandgap ranging from 2.1 to 2.6 eV [48], enabling effective absorption of a significant portion of the solar spectrum. CuO, on the other hand, possesses a direct bandgap of approximately 1.2 to 1.7 eV [49]. Both materials are prone to photo-corrosion, as the photo-generated electron-hole pairs often participate in reducing the copper oxides rather than driving the HER. To address the issue of photo-corrosion, Kalanur *et al.* [22] proposed a multijunction approach (**Figure 2 (a-f)**). Their study involved incorporating a layer of Cu_2O with a carefully designed hole extraction layer composed of a non-noble metal material, NiO_x. Furthermore, an aluminium-doped zinc oxide (AZO) layer was added as an electron tunnelling layer on top of the Cu_2O (**Figure 2 (a, c)**). This encapsulation technique significantly inhibits photo-corrosion. To further enhance performance, a non-toxic MoO_x catalyst layer was integrated into the multijunction structure. The resulting $NiO_x/Cu_2O/AZO/MoO_x$ photocathode demonstrated an impressive photocurrent density of 6.1 mA cm^{-2} at 0 V *vs* RHE and exhibited minimal decay in photocurrent during a 6-hour stability test (**Figure 2 (e)**) and showed maximum incident to photon conversion efficiency (IPCE) of about ~60% until 500 nm (**Figure 2 (f)**). This approach represents a significant advancement in photocathode construction, as it enables non-noble metal materials to extract holes, facilitate electron tunnelling, and co-catalyse the HER, achieving performance comparable to noble metal-integrated counterparts.

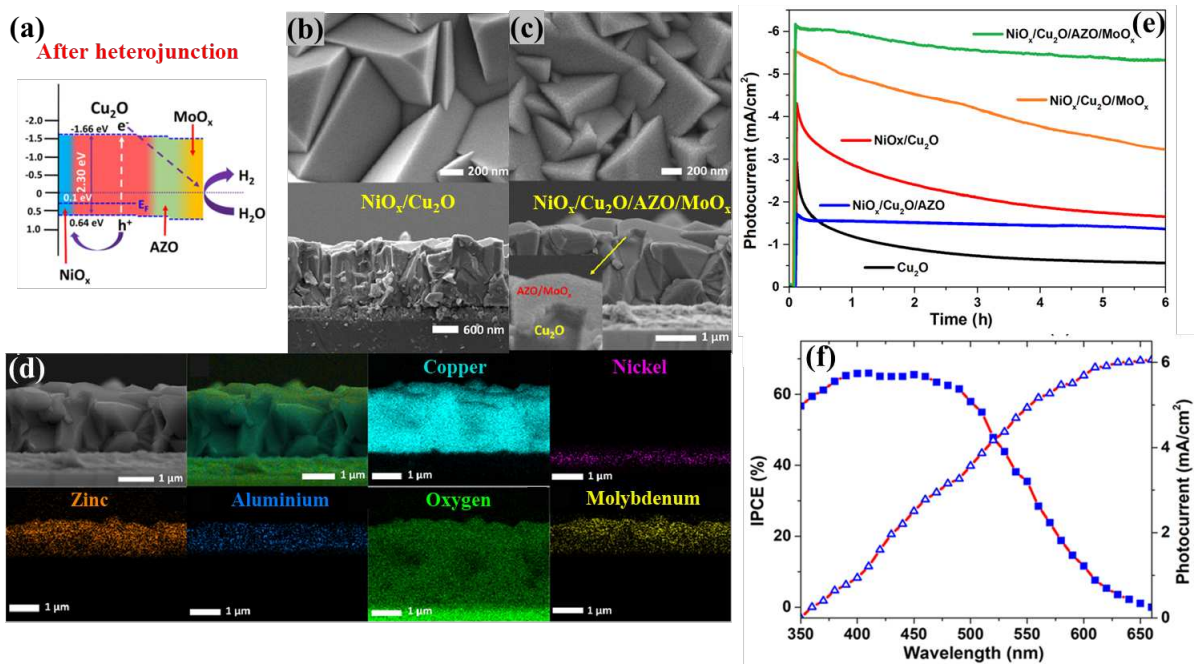

Figure 2. (a) Formation of heterojunction along with the photogenerated carriers dynamics on FTO/NiO_x/Cu_2O/MoO_x. FESEM images of **(b)** NiOx/Cu_2O and **(c)** NiO_x/Cu_2O/AZO/MoO_x on FTO substrate. **(d)** HAADF and Elemental mapping of all elements. **(e)** Long-term stability of all prepared electrodes. **(f)** IPCE plots of NiO_x/Cu_2O/AZO/MoO_x. Reproduced with permission [22], Copyright 2022, Elsevier.

CO_3O_4 (cobaltosic oxide) is another semiconducting material that has received significant attention in recent research due to its favourable electronic and optical properties, as well as its long-term chemical stability. With an energy gap ranging from 1.5 to 2.6 eV [24], CO_3O_4 can efficiently absorb visible light, making it a promising candidate for hydrogen production via water splitting. However, there are challenges associated with using CO_3O_4 as a photocathode, including its relatively high overpotentials ranging from 400 mV to 600 mV in alkaline solutions (i.e., KOH). To overcome these limitations using sustainable non-noble metal materials, researchers like Abdelmoneim *et al.* have explored doping techniques [26]. They successfully co-doped CO_3O_4 with nickel (Ni) and iron (Fe), resulting in a 6% (Fe, Ni) CO_3O_4 electrode. This modified electrode exhibited a significant cathodic photocurrent density of 13.6 mA cm^{-2} at -1V *vs* RHE and a solar-to-hydrogen conversion efficiency of approximately 11.3% [26]. These findings offer promising possibilities for further

advancements in the utilization of CO_3O_4 as a photocathode material, with the potential for even better performance without the need for noble metal incorporation.

Another metal oxide of significant interest is NiO. It is commonly utilized as a hole-selective layer in many photocathodes due to its suitable bandgap and band alignment [50]. However, its performance in hydrogen reduction during water splitting has been less impressive compared to other metal oxide photocathodes due to relatively high rates of charge recombination. To tackle this challenge, Sahoo *et al.* implemented a doping strategy by introducing monovalent metals, specifically copper, into NiO. This doping resulted in improved physical properties and yielded a modest cathodic photocurrent density of 6.97 mA cm^{-2} at 0 V *vs* RHE. The enhancement was attributed to a reduction in charge transfer resistance observed in electrochemical impedance spectroscopy (EIS) measurements, indicating enhanced separation of photogenerated charge carriers after copper doping [27]. Another study by Song *et al.* investigated the use of such copper-doped nickel oxide (Cu:NiO) layer as a hole-selective back contact material for the primary semiconductor $CuBi_2O_4$. The combination of the thin Cu:NiO layer with $CuBi_2O_4$ exhibited a synergistic effect, significantly improving the cathodic photocurrent density. Specifically, they achieved a cathodic photocurrent density of 2.83 mA cm^{-2} at 0.6 V *vs* RHE [28]. This improvement is noteworthy considering that $CuBi_2O_4$ typically demonstrates low charge carrier mobility, which hinders efficient extraction and transport of photoexcited charges [29].

2.2. Metal chalcogenide-based photocathodes

Metal chalcogenides have attracted significant attention as photocathode materials due to their distinctive electronic and optical properties. These materials consist of one or more electropositive elements combined with at least one chalcogen anion, such as Sulfur (S), Selenium (Se), or Tellurium (Te). The composition of metal chalcogenides results in unique energy bands that make them suitable for various applications. By adjusting the metal and

chalcogenide components, it is possible to tune the bandgaps according to specific requirements. Moreover, many metal chalcogenides have direct bandgaps, enabling efficient absorption of a wide range of wavelengths and promoting high photocurrent generation while minimizing energy losses. However, several challenges exist in utilizing metal chalcogenides for PEC HER, including instability, slow reaction kinetics, charge recombination, and performance degradation caused by surface oxidation and corrosion during harsh water-splitting processes [51]. Researchers have been working to address these limitations. For example, Guo *et al.* developed high-quality films of Sb_2Se_3 with surface morphologies composed of nanorod (NR) arrays using a cost-effective and scalable close-spaced sublimation technique (**Figure 3(a, b)**). They further improved the performance by sputtering a non-precious and scalable crystalline molybdenum sulfide (MoS_2) film as a cocatalyst and protective layer on the Sb_2Se_3 NR arrays (**Figure 3 (c-g)**). The resulting core-shell structured MoS_2/Sb_2Se_3 NR PEC devices achieved an impressive photocurrent density of 10 mA cm^{-2} at 0 V *vs* RHE under simulated solar light [30]. The enhanced performance (**Figure 3 (h)**) of the photocathode was attributed to the effective charge transfer facilitated by the reduced charge transfer resistance also observed in the EIS results (**Figure 3 (i)**). This was achieved through the synergistic effect of the photocathode's structure (**Figure 3 (a, b)**). The role of MoS_2 as a cocatalyst should not be underestimated, as it has demonstrated remarkable performance, even surpassing that of Pt in photocatalytic applications [52]. Depending on its phase, whether in the 2H semiconducting phase or the 1T metallic phase, or a combination of both, MoS_2 can be incorporated to fulfil specific requirements. It can act as a semiconductor, forming junctions with other semiconductors if desired, or function similarly to a metallic cocatalyst like Pt. This versatility was also utilized by Hu *et al.*, who hydrothermally loaded a mixture of 1T and 2H phase MoS_2 onto a hydrogenated anatase/rutile hetero-phase TiO_2 to create a new MoS_2/TiO_2 photocathode. The resulting cathodic photocurrent density of MoS_2/TiO_2 reached 5.2 mA cm^{-2},

which was approximately 2.7 times higher than that of a Pt-loaded TiO_2 photocathode achieving 1.9 mA cm^{-2} in similar conditions [31].

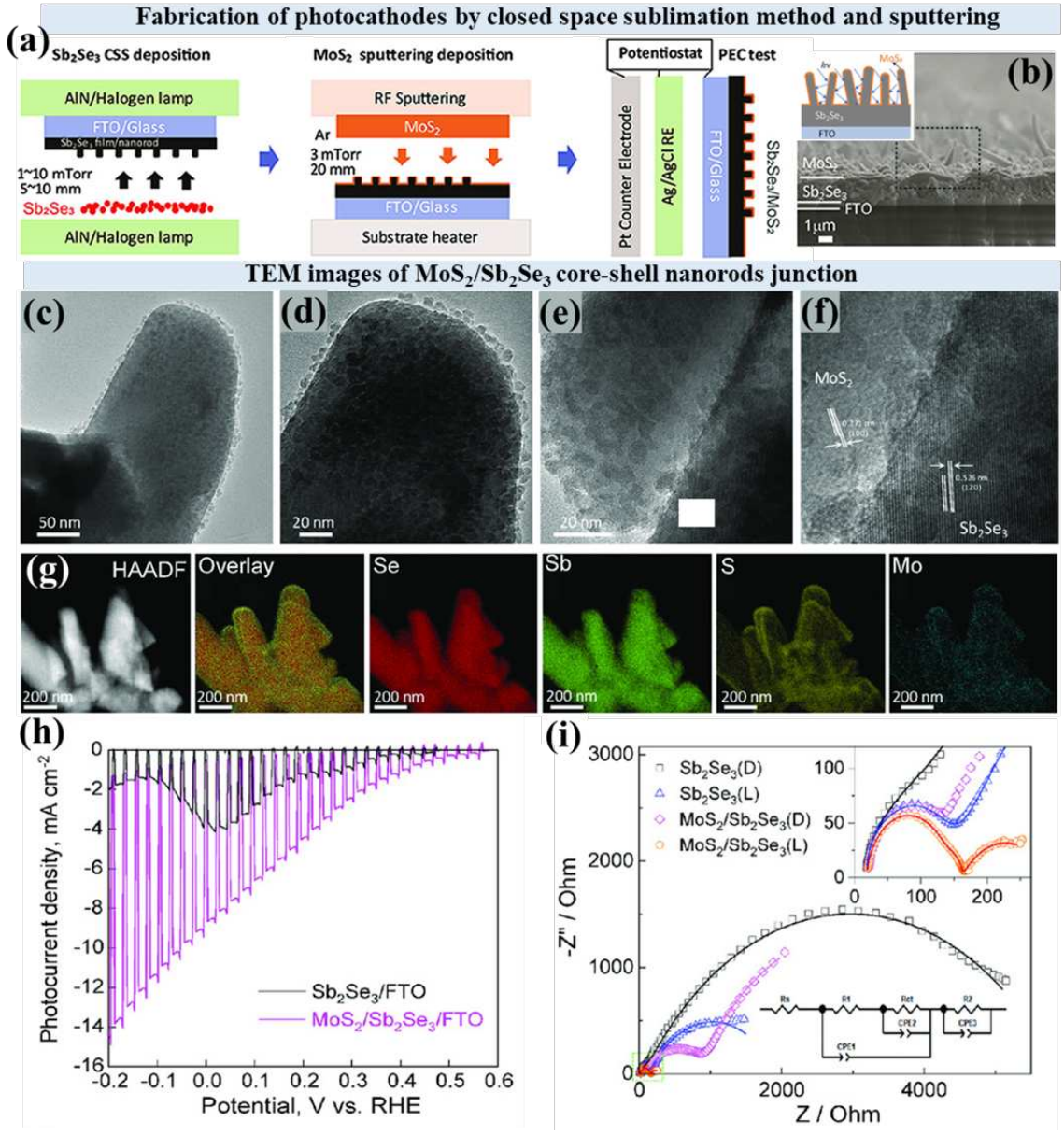

Figure 3. (a) Fabrication process of core-shell MoS_2/Sb_2Se_3 nanorods (NR) array electrodes by closed space sublimation (CSS) method and sputtering. **(b)** Cross-sectional SEM image of MoS_2/Sb_2Se_3 photocathodes. **(c-f)** HRTEM images of prepared core-shell MoS_2/Sb_2Se_3 NR interface. **(g)** Elemental mapping of prepared photocathodes. **(h)** Linear sweep voltammetry of bare Sb_2Se_3 and 30 nm MoS_2/Sb_2Se_3 photocathodes under AM 1.5G illumination. **(i)** Nyquist plots of Sb_2Se_3 and core-shell MoS_2/Sb_2Se_3 NR electrodes at 0V vs RHE under dark and illumination conditions. Reproduced with permission [30]. Copyright 2020, John Wiley & Sons.

The chalcogenide compound $Cu_2BaSn(S,Se)_4$, also known as CBTSSe, has gained significant attention as a photocathode for water splitting, similar to other chalcogenides like

$Cu_2ZnSn(S,Se)_4$ (CZTSSe) [53, 54]. These materials have attracted interest because they utilize abundant elements such as copper, zinc, and tin in their structures, making them cost-effective and potentially suitable for large-scale hydrogen production. CBTSSe photocathodes have a desirable direct band gap ranging from 1.5 to 2.0 eV, which makes them well-suited for HER, especially when compared to CZTSSe photocathodes that have inherent anti-site defects [32, 55]. When combined with sustainable cocatalysts or modified with abundant elements, they have the potential to enable economically viable hydrogen production through water reduction. A study conducted by Xie *et al.* demonstrated promising results using molybdenum (Mo)-coated quartz substrates to apply a precursor solution, followed by annealing with sublimated sulfur to create Mo/CBTS photocathodes. They achieved a cathodic photocurrent of 4 mA cm^{-2} at 0 V *vs* RHE. The excellent performance of the photocathodes was attributed to the coated Mo and the large grain sizes of the resulting structures, which reduce charge recombination as grain boundaries and defects would otherwise promote recombination. These findings offer a pathway to unlock the full potential of these photocathodes by integrating other abundant and efficient HER materials, like MoS_x to achieve the maximum theoretical photocurrents for this material [33].

Several other metal chalcogenides have demonstrated potential as photocathodes for water splitting without needing noble metal incorporation. These include Cu_2S [34, 35], and ternary chalcogenides such as Cu_3BiS_3 [37] and $CuInS_2$ [38]. When combined with non-noble metal materials, such as cocatalysts like CoP [56] or semiconducting protective layers like ZnO [34, 35] that serve as sites for electron mobility after junction formation, improved photocathodes can be developed.

2.3. Metal phosphide based photocathodes

Cobalt phosphide with its different phases, CoP and Co_2P, serves a dual role as a cocatalyst for the HER and as a protective layer for unstable primary semiconductors, shielding them from corrosion when in direct contact with an electrolyte solution [57]. They exhibit high catalytic activity comparable to that of platinum (Pt). In a study conducted by Thalluri *et al.*, Co_2P was employed to significantly enhance the photocurrent production of p-type silicon (p-Si), resulting in an impressive photocurrent density of 35.2 mA cm^{-2} at 0 V *vs* RHE[39].

This performance rivalled that of other silicon photocathodes incorporating junctions for passivation and Pt as the HER catalyst. The enhancement was achieved through a series of steps and the advantage of thickness gradient in the inverted pyramid configuration is given in **Figure 4 (a)**. First, galvanostatic electrochemical etching was performed on the p-Si surface (**Figure 4 (b)** and inset) to create a pyramid texture. Then, Co_2P was gradient deposited on the textured surface (**Figure 4 (c, d)**), effectively reducing parasitic energy losses by separating the catalytic sites from the light absorption sites through the controlled distribution of Co_2P loading. This configuration exhibited remarkable stability, maintaining its photocurrent density even with prolonged operation (**Figure 4 (k)**). When Pt was used as a replacement for the optimized Co_2P loading under the same conditions, its performance was found to be significantly inferior (**Figure 4 (l)**) [38].

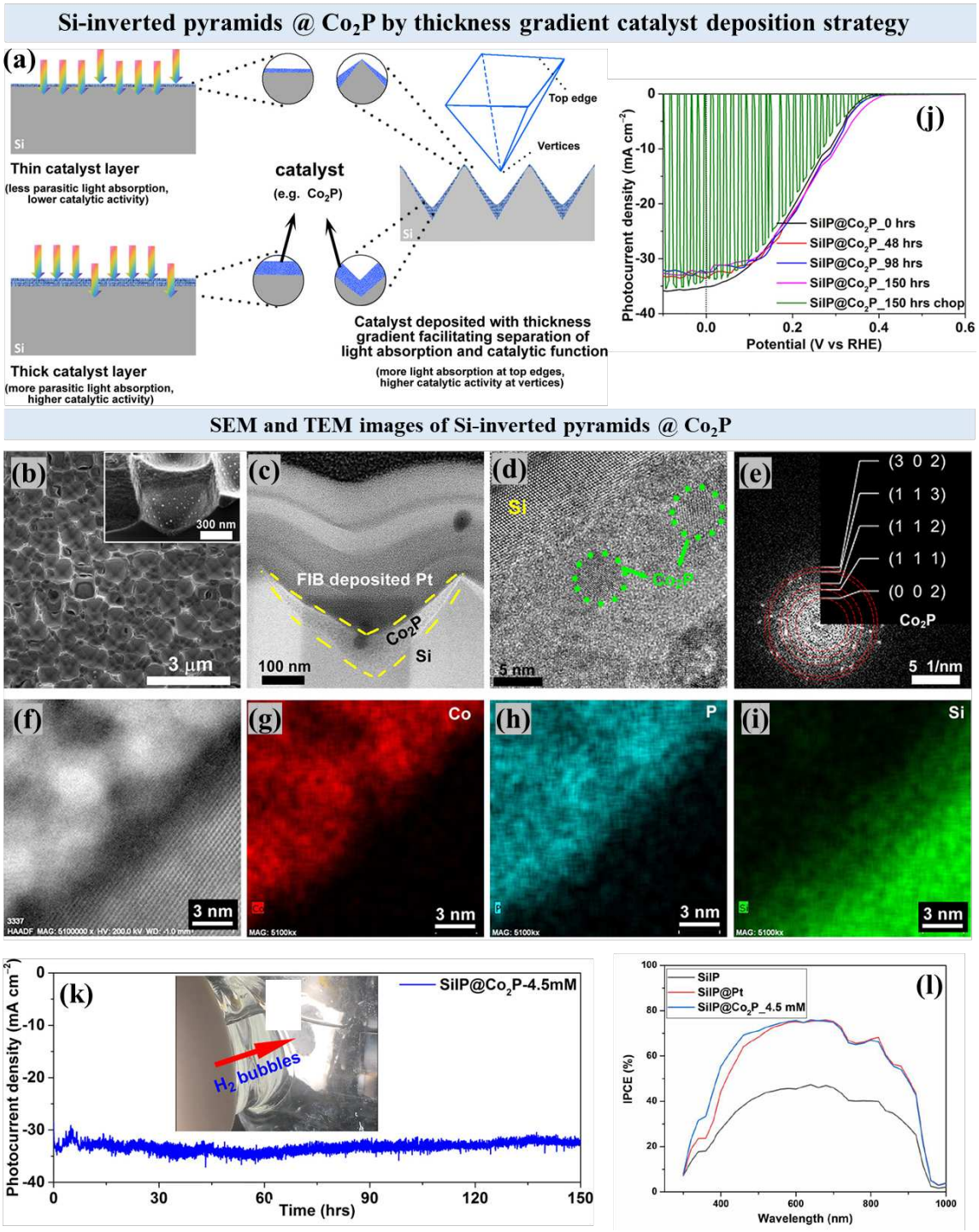

Figure 4. (a) Influence of catalyst layer thickness on light absorption and advantages of thickness gradient catalytic layer in the inverted pyramid configuration. **(b)** SEM image of Si-inverted pyramid @ Co_2P 4.5mM photocathodes. **(c)** Cross-sectional TEM image showing Co_2P in Si-IP. **(d)** HRTEM images showing the crystalline structure of Co_2P (e) FFT-ED pattern of Co_2P layer on Si-IP configuration. **(f-i)** HAADF and elemental maps of Co, P, Si. **(j)** LSV taken before and after long-term stability test with varied time intervals. **(k)** Long-term stability (I-T curve) of prepared Co_2P @Si-IP photocathodes measured at 0 V vs RHE under AM 1.5G illumination. **(l)** IPCE curve of all prepared photocathodes measured at -1 V in 0.5M H_2SO_4 electrolyte. Reproduced with permission [39]. Copyright 2019, American Chemical Society.

Other metal phosphides, such as GaP [40] and $GaInP_2$ [58], have demonstrated potential in generating high photocurrents when combined with non-noble metal materials and modified accordingly. In the case of $GaInP_2$, when coupled with thin films of MoS_2 that serve as both a catalyst and a protective layer, it achieves performance comparable to that of a platinum.

2.4. Silicon-based photocathodes

Silicon-based photocathodes have consistently attracted significant attention for their potential in water reduction to produce environmentally friendly hydrogen. Silicon (Si) is a cost-effective and readily available semiconductor material with desirable electronic properties. Among silicon-based photocathodes, p-type silicon has been the focus of most research, despite its inherent sluggish kinetics for the HER [41]. Recent studies for this material have aimed to develop photocathode designs using abundant materials that can rival or surpass the performance of noble metals. One such study conducted by Lin *et al.* employed a facile assembly process to create an amorphous thin film of MoS_x on p-Si, resulting in a remarkable cathodic photocurrent density of 28.2 mA cm^{-2} at 0 V *vs* RHE, accompanied by a high Faradaic efficiency of approximately 98% [42]. Similar trends are observed in other studies that utilize non-noble metal-based materials to form efficient heterojunctions with p-Si. For instance, Ku *et al.* achieved a powerful Schottky junction by integrating 3D textured graphene onto p-Si. This integration enhanced electrochemical activity, stability, and charge separation efficiency, leading to an impressive cathodic photocurrent density of 32.5 mA cm^{-2} at 0 V *vs* RHE [43]. These results indicate the tremendous potential of silicon-based photocathodes for water splitting and hydrogen production. The theoretical limit of their photocurrent has not yet been reached, definitely leaving room for further improvement.

2.5. Metal-free photocathodes

Metal-free photocathodes composed of carbon-based semiconductor materials, such as graphene oxide [44] and graphitic carbon nitride (g-C_3N_4) [45, 59], have been investigated as

highly active and cost-effective alternatives. These photocathodes are synthesized using various methods, including thermal treatment, hydrothermal synthesis, and solvothermal synthesis. Similar to other photocathode designs that utilize p-n junctions by integrating p-type and n-type semiconductors for charge separation and as passivation layers for stability, these carbon-based materials also play a similar role due to their favourable electrical and optical properties. In a study by Ma *et al.*, three-dimensional Cu_2O foams, which outperform Cu_2O films, are coated with g-C_3N_4 to enhance stability and photocurrent generation. The resulting composite photocathode achieves a cathodic photocurrent density of 2.5 mA cm^{-2} at 0 V *vs* RHE [46], representing a modest improvement brought by better electron mediation within the photocathode.

3. Conclusion and outlook

A diverse range of non-noble metal-based materials has emerged as promising photocathodes for water splitting, exhibiting remarkable performance in HER. Metal phosphides, such as CoP, have demonstrated exceptional catalytic activity for HER while simultaneously serving as passivation layers, shielding vulnerable primary semiconductors from corrosion. These materials have achieved competitive photocurrent densities, rivalling or even surpassing those of Pt-based photocathodes. Carbon-based semiconductors, including graphene oxide and graphitic carbon nitride, hold immense potential due to their exceptional stability, however, further research is warranted to fully harness their capabilities. Similarly, significant advancements have been made in the utilization of metal chalcogenides. When combined with non-noble metal materials or modified with abundant elements, these materials have exhibited potential for efficient and cost-effective hydrogen production. Silicon-based photocathodes stand out as particularly promising material technologies for clean energy production through PEC water splitting due to their exceptional efficiency in converting sunlight illumination into electric current, resistance to corrosion and degradation over

extended operation periods, and relatively low production costs. Non-noble plasmonic metal-based photocatalysts, such as copper (Cu), aluminium (Al), and nickel (Ni), exhibit plasmon resonance effects, a phenomenon where collective oscillations of electrons are induced by incident light, leading to enhanced light absorption and scattering, ultimately resulting in localized electromagnetic field enhancement [60]. Researchers have made significant strides too in the development and optimization of these materials through meticulous synthesis methods tailored to improve surface modifications, ultimately enabling hybridization with non-noble metal semiconductors for HER water splitting.

The outlook for non-noble metal-based photocathodes for water splitting is decidedly optimistic. The rapid advancements in non-noble metal-based photocathodes, some with performances already surpassing those of their noble metal counterparts, mark a pivotal moment in the evolution of PEC water splitting technology. These promising alternatives have the potential to propel PEC hydrogen production towards greater scalability and widespread adoption. Ongoing research endeavours continue to aim for optimization of the performance, stability, and scalability of these photocathodes through various discussed strategies, including surface modification, heterojunction formation, and nano-structuring. By leveraging these abundant and sustainable materials, non-noble metal-based photocathodes will play a pivotal role in realizing a clean and renewable energy future.

CRediT authorship contribution statement

Antony Charles Minja: Conceptualization, Writing – original draft, Writing- review & editing, **Karthick Raj AG:** Conceptualization, Writing – original draft, Writing – review & editing, **Arno Raes:** Writing review & editing, **Rituraj Borah:** Writing- review & editing, **Sammy W. Verbruggen:** Conceptualization, Funding acquisition, Supervision, Writing-review & editing.

Declaration of competing interest

The authors declare no competing financial interests.

Acknowledgements

A.C.M. and S.W.V. kindly acknowledge the University of Antwerp Special Research Fund for a DOCPRO4 doctoral fellowship (FFB210298).

Corresponding Author

Email: Sammy.verbruggen@uantwerpen.be

References and recommended reading

Papers of particular interest, published within the period of review, have been highlighted as:

* of special interest

** of outstanding interest

1. Panchenko, V., et al., *Prospects for the production of green hydrogen: Review of countries with high potential.* International Journal of Hydrogen Energy, 2023. **48**(12): p. 4551-4571.
2. Esposito, D.V., *Membraneless electrolyzers for low-cost hydrogen production in a renewable energy future.* Joule, 2017. **1**(4): p. 651-658.
3. Gopannagari, M., et al., *High-Performance Silver-Doped Porous CuBi2O4 Photocathode Integrated with NiO Hole-Selective Layer for Improved Photoelectrochemical Water Splitting.* Advanced Sustainable Systems, 2023. **7**(8): p. 2300085.
4. Wang, P., et al., *Decorating Cu2O photocathode with cu/Al bimetallic layer for enhanced photoelectrochemical water splitting.* International Journal of Energy Research, 2022. **46**(12): p. 16991-17002.

5. Mao, G., et al., *WO3@ Fe2O3 Core-Shell Heterojunction Photoanodes for Efficient Photoelectrochemical Water Splitting.* Chinese Journal of Structural Chemistry, 2022. **41**(8): p. 2208025-2208030.

6. Zhang, H., et al., *Recent Advances on Small Band Gap Semiconductor Materials (≤ 2.1 eV) for Solar Water Splitting.* Catalysts, 2023. **13**(4): p. 728.

7. Yu, R., et al., *Decorating Cu2O with Ni-doped metal organic frameworks as efficient photocathodes for solar water splitting.* International Journal of Hydrogen Energy, 2023. **48**(45): p. 17065-17073.

8. Zhang, F., et al., *Multistage charge redistribution constructing heterostructured WO3@ RuSe2 on Si for enhanced photoelectrochemical hydrogen evolution.* Chemical Engineering Journal, 2022. **446**: p. 137462.

9. Cheng, S., et al., *Synergism of 1D CdS/2D modified Ti3C2Tx Mxene heterojunctions for boosted photocatalytic hydrogen production.* Chinese Journal of Structural Chemistry, 2022. **41**(8): p. 2208058-2208064.

10. Park, J., et al., *Hierarchal nanorod-derived bilayer strategy to enhance the photocurrent density of Sb2Se3 photocathodes for photoelectrochemical water splitting.* ACS Energy Letters, 2019. **5**(1): p. 136-145.

11. Yang, W., et al., *Benchmark performance of low-cost Sb2Se3 photocathodes for unassisted solar overall water splitting.* Nature communications, 2020. **11**(1): p. 861.

*12. Chen, Y.-C., et al., *Solution–processed Cu2O/ZnO/TiO2/Pt nanowire photocathode for efficient photoelectrochemical water splitting.* Journal of Alloys and Compounds, 2022. **899**: p. 163348.

This work highlights the simple synthesis methods used to create a high-performing noble-metal based electrode that can be produced at large scale. This provides insights to researchers on how to develop non-noble metal counterparts.

13. Tong, S., et al., *Single atom catalysts for boosting electrocatalytic and photoelectrocatalytic performances.* Journal of Materials Chemistry A, 2021. **9**(17): p. 10731-10738.

14. Lee, J. and J. Oh, *Nanopixelated cuprous oxide photocathodes for durable photoelectrochemical water splitting.* ACS Energy Letters, 2022. **7**(10): p. 3244-3250.

*15. Zhang, X., et al., *Solution-Processed Cu2S Nanostructures for Solar Hydrogen Production.* Chemistry of Materials, 2023. **35**(6): p. 2371-2380.

The authors present a simple, inexpensive, and efficient method to produce pure-phase nanostructured Cu_2S thin films for large-scale solar hydrogen production at average current generation levels.

16. Adams, P., et al., *Solution phase treatments of Sb 2 Se 3 heterojunction photocathodes for improved water splitting performance.* Journal of Materials Chemistry A, 2023. **11**(15): p. 8277-8284.

17. Yi, S.-S., et al., *Non-noble metals applied to solar water splitting.* Energy & Environmental Science, 2018. **11**(11): p. 3128-3156.

*18. Wang, Q., et al., *Stability of Photocathodes: A Review on Principles, Design, and Strategies.* ChemSusChem, 2023: p. e202202186.

This review comprehensively examines the development of noble metal- and non-noble metal-based photocathodes, including all enhancement strategies and their effects.

*19. Tan, J., et al., *Surface restoration of polycrystalline Sb2Se3 thin films by conjugated molecules enabling high-performance photocathodes for photoelectrochemical water splitting.* Applied Catalysis B: Environmental, 2021. **286**: p. 119890.

This article shows how to use conjugated molecules to restore the surface of polycrystalline thin films, which enables high onset potential, photocurrent density, and half-cell solar-to-hydrogen efficiency. This is achieved by designing the band gap and alignment of the materials to improve performance.

20. Wang, Y., et al., *Improving the p–type conductivity of Cu2O thin films by Ni doping and their heterojunction with n–ZnO.* Applied Surface Science, 2022. **590**: p. 153047.

21. Wu, H., et al., *A pulse electrodeposited amorphous tunnel layer stabilises Cu 2 O for efficient photoelectrochemical water splitting under visible-light irradiation.* Journal of Materials Chemistry A, 2020. **8**(11): p. 5638-5646.

22. Kalanur, S.S., Y.J. Lee, and H. Seo, *Enhanced and stable photoelectrochemical H2 production using a engineered nano multijunction with Cu2O photocathode.* Materials Today Chemistry, 2022. **26: p. 101031.

This article showcases improvement in the efficiency of charge separation and stability of the Cu_2O photocathode by employing a multi-layer approach involving precisely adjusted layers of NiO_x, aluminium doped zinc oxide (AZO), and MoO_x.

23. Shinde, P., et al., *Synthesis of MoS 2 from [Mo 3 S 7 (S 2 CNEt 2) 3] I for enhancing photoelectrochemical performance and stability of Cu 2 O photocathode toward efficient solar water splitting.* Journal of Materials Chemistry A, 2018. **6**(20): p. 9569-9582.

24. Moridon, S.N.F., et al., *Cobalt oxide as photocatalyst for water splitting: Temperature-dependent phase structures.* International Journal of Hydrogen Energy, 2019. **44**(47): p. 25495-25504.

25. Ebadi, M., et al., *Electrodeposited p-type Co 3 O 4 with high photoelectrochemical performance in aqueous medium.* RSC Advances, 2015. **5**(46): p. 36820-36827.

26. Abdelmoneim, A., et al., *Outstanding stability and photoelectrochemical catalytic performance of (Fe, Ni) co-doped Co3O4 photoelectrodes for solar hydrogen production.* International Journal of Hydrogen Energy, 2021. **46**(24): p. 12915-12935.

27. Sahoo, P., et al., *Cu doped NiO thin film photocathodes for enhanced PEC performance.* Superlattices and Microstructures, 2021. **159**: p. 107050.

28. Song, A., et al., *Cu: NiO as a hole-selective back contact to improve the photoelectrochemical performance of CuBi 2 O 4 thin film photocathodes.* Journal of Materials Chemistry A, 2019. **7**(15): p. 9183-9194.

29. Monny, S.A., et al., *Fabricating highly efficient heterostructured CuBi 2 O 4 photocathodes for unbiased water splitting.* Journal of Materials Chemistry A, 2020. **8**(5): p. 2498-2504.
30. Guo, L., et al., *Scalable core–shell MoS2/Sb2Se3 nanorod array photocathodes for enhanced photoelectrochemical water splitting.* Solar RRL, 2020. **4**(3): p. 1900442.
31. Hu, J., et al., *MoS2 supported on hydrogenated TiO2 heterostructure film as photocathode for photoelectrochemical hydrogen production.* International Journal of Hydrogen Energy, 2019. **44**(59): p. 31008-31019.
32. Sharma, A., et al., *Visible-light induced photosplitting of water using solution-processed Cu2BaSnS4 photoelectrodes and a tandem approach for development of Pt-free photoelectrochemical cell.* Materials Science in Semiconductor Processing, 2021. **121**: p. 105433.
33. Xie, J., et al., *Large-grained Cu2BaSnS4 films for photocathodes.* ACS Applied Materials & Interfaces, 2019. **11**(36): p. 33102-33108.
34. Luo, S., et al., *3D hierarchically branched Cu2S/ZnO heterojunction nanowire arrays for enhanced solar water splitting.* Materials Today Communications, 2023. **34**: p. 105417.
35. Fu, S., et al., *Enhanced photo-electrochemical activity of ZnO/Cu2S nanotube arrays photocathodes.* International Journal of Hydrogen Energy, 2021. **46**(21): p. 11544-11555.
36. Wu, Y., et al., *Colloidal synthesis of SnS nanocrystals with dimension-dependent photoelectrochemical properties.* New Journal of Chemistry, 2019. **43**(19): p. 7457-7462.

37. Moon, S., et al., *Bi2S3-Cu3BiS3 Mixed Phase Interlayer for High-Performance Cu3BiS3-Photocathode for 2.33% Unassisted Solar Water Splitting Efficiency.* Advanced Science, 2023. **10(6): p. 2206286.

The authors used a one-step solution processing technique to place Bi2S3 onto Cu_3BiS_3. This approach effectively showcased a stable and efficient photocathode based on Cu_3BiS_3, capable of performing solar water splitting without the need for an external bias.

38. Chae, S.Y., et al., *Monitoring Transformations of Catalytic Active States in Photocathodes Based on MoSx Layers on CuInS2 Using In Operando Raman Spectroscopy.* Angewandte Chemie, 2023. **135(7): p. e202215227.

Operando Raman spectroscopy uncovered the activation process of $CuInS_2/MoS_x$ for producing hydrogen through PEC reactions. This research provides valuable understanding of the transitional stages involved in activation, contributing to a deeper comprehension of PEC processes.

39. Thalluri, S.M., et al., *Inverted pyramid textured p-silicon covered with Co2P as an efficient and stable solar hydrogen evolution photocathode.* ACS energy letters, 2019. **4**(7): p. 1755-1762.

40. Xu, Z., et al., *Direct In Situ Measurement of Quantum Efficiencies of Charge Separation and Proton Reduction at TiO2-Protected GaP Photocathodes.* Journal of the American Chemical Society, 2023. **145**(5): p. 2860-2869.

41. Meng, L., et al., *Ni/Fe codoped In2S3 nanosheet arrays boost photo-electrochemical performance of planar Si photocathodes.* Advanced Energy Materials, 2019. **9**(38): p. 1902135.

42. Lin, H., et al., *In situ assembly of MoSx thin-film through self-reduction on p-Si for drastic enhancement of photoelectrochemical hydrogen evolution.* Advanced Functional Materials, 2021. **31(3): p. 2007071.

A uniform layer of amorphous MoS_x thin film was created through a self-reduction process involving cyclic formation. This distinctive structure of the photocathode, combining a-MoS_x with p-Si, gives an impressive cathodic current density of 28.2 mA cm^{-2} at 0 *vs* RHE.

43. Ku, C.K., et al., *Creation of 3D Textured Graphene/Si Schottky Junction Photocathode for Enhanced Photo-Electrochemical Efficiency and Stability.* Advanced Energy Materials, 2019. **9**(29): p. 1901022.

44. Farahi, M., et al., *A novel Z-scheme heterojunction g-C3N4/WS2@ rGONR (x) nanocomposite for efficient photoelectrochemical water splitting.* Materials Chemistry and Physics, 2023. **293**: p. 126941.

*45. Wang, Z., et al., *Rationally Designed Copper-Modified Polymeric Carbon Nitride as a Photocathode for Solar Water Splitting.* ChemSusChem, 2019. **12**(4): p. 866-872.

The authors used copper-modified polymeric carbon nitride as a photocathode material. This design improved the slow charge separation kinetics of polymeric carbon nitride, resulting in a better photocathode.

46. Ma, X., et al., *Hierarchical Cu2O foam/g-C3N4 photocathode for photoelectrochemical hydrogen production.* Applied Surface Science, 2018. **427**: p. 907-916.

47. Sundararaj, S.B., et al., *Interfacial charge separation of nickel tungstate anchored on g-C3N4 heterojunction stimulates visible-light driven direct Z-scheme photoelectrochemical hydrogen evolution.* International Journal of Hydrogen Energy, 2023.

48. Visibile, A., et al., *Influence of strain on the band gap of Cu2O.* Chemistry of Materials, 2019. **31**(13): p. 4787-4792.

49. Siavash Moakhar, R., et al., *Photoelectrochemical water-splitting using CuO-based electrodes for hydrogen production: a review.* Advanced Materials, 2021. **33**(33): p. 2007285.

50. Wei, Y., et al., *A low-cost NiO hole transfer layer for ohmic back contact to Cu2O for photoelectrochemical water splitting.* Small, 2017. **13**(39): p. 1702007.

51. Ros, C., et al., *Turning Earth abundant Kesterite-based solar cells into efficient protected water-splitting photocathodes.* ACS applied materials & interfaces, 2018. **10**(16): p. 13425-13433.

52. Liu, Y., et al., *2H-and 1T-mixed phase few-layer MoS2 as a superior to Pt co-catalyst coated on TiO2 nanorod arrays for photocatalytic hydrogen evolution.* Applied Catalysis B: Environmental, 2019. **241**: p. 236-245.

53. Song, J., et al., *Porous Cu2BaSn (S, Se) 4 Film as a Photocathode Using Non-Toxic Solvent and a Ball-Milling Approach.* ACS Applied Energy Materials, 2021. **4**(1): p. 81-87.

54. Liang, G., et al., *Charge Separation Enhancement Enables Record Photocurrent Density in Cu2ZnSn (S, Se) 4 Photocathodes for Efficient Solar Hydrogen Production.* Advanced Energy Materials, 2023. **13(19): p. 2300215.

This study attains an impressive photocurrent density of 40.40 mA cm^{-2} (measured at 0 *vs* RHE), nearing its theoretical limit of 42.85 mA cm^{-2}. This achievement stands as the highest recorded value for photocathodes based on kesterites.

55. Mkawi, E., et al., *Fabricating chalcogenide Cu2ZnSnS4 (CZTS) nanoparticles via solvothermal synthesis: Effect of the sulfur source on the properties.* Ceramics International, 2020. **46**(16): p. 24916-24922.

56. Yang, Y., et al., *Design and synthesis Zn doped CoP/Co2P nanowire arrays for boosting hydrogen generation reaction.* Journal of Solid State Chemistry, 2020. **285**: p. 121231.

57. Zhang, J., et al., *In situ growth of Co2P nanocrystal on g-C3N4 for efficient and stable photocatalytic hydrogen evolution.* Energy & Fuels, 2021. **35**(2): p. 1859-1865.

58. Britto, R.J., et al., *Interfacial engineering of gallium indium phosphide photoelectrodes for hydrogen evolution with precious metal and non-precious metal based catalysts.* Journal of Materials Chemistry A, 2019. **7**(28): p. 16821-16832.

59. Wen, P., et al., *In situ decorated Ni 2 P nanocrystal co-catalysts on gC 3 N 4 for efficient and stable photocatalytic hydrogen evolution via a facile co-heating method.* Journal of Materials Chemistry A, 2020. **8**(6): p. 2995-3004.
60. Sayed, M., et al., *Non-noble plasmonic metal-based photocatalysts.* Chemical Reviews, 2022. **122**(11): p. 10484-10537.